International Journal of Scientific and Technological Research
ISSN 2422-8702 (Online)
Vol 4, No.4, 2018

Vibration Properties of TPMS Based Structures

Gokhan Altintas
Manisa Celal Bayar University, Department of Civil Engineering, Mechanics Division
Sehit Prof. Dr. Ilhan Varank Campus, 45140, Manisa, Turkey
E-mail: gokhan.altintas@cbu.edu.tr

Abstract

Having interesting properties, inherent characteristics and certain trigonometric function compositions, TPMSs (triply periodic minimal surfaces), is one of the best candidate for porous scaffold production by having many tuneable parameters. TPMS unit cells have a crystalline structure, in the sense of repeating themselves infinitely in space, in other words being triply periodic. The structure can be found in living beings such as butterflies, beetles and other insects as biologically optimized surfaces for different focuses. TPMS based scaffolds can be optimized for not only geometric but also mechanic requirements by tunning parameters. Besides to tunable parameters, the development of 3D printer systems that can use metalic materials, it has become possible to produce porous structures that can be obtained with increased precision of micro details for the productions requiring certain mechanical properties.

In this study, the natural vibrational behavior of TPMS based structures is investigated by focusing on the combination of material and geometry with the highest production potential. TPMS structures with different geometry, material and wall thickness have been studied in a wide and feasible range depending on the change of parameters directly affecting modal behavior such as mass and stiffness. In this respect, the results that can be used as comparative values for TPMS based constructions are obtained. As a result of the obtained results, it has been seen that not only the numerical changes in the natural vibration behaviors of the systems, but also the behavioral characteristics which are difficult to predict are emerged. It is thought that the results obtained are important not only for theoretical studies but also for practical applications.

Keywords: Triply periodic, minimal surfaces, natural vibration, TMPS, modal analysis

1. Introduction

Scaffolds with interconnected pore structures have a wide use potential due to their mechanical properties and their use in mass and heat transfer applications. Scaffold usage in engineering for optimum performance must commence by quantitatively determination of scaffold necessities through specific properties. Regardless of production technique, it is desirable to compute effective scaffold properties like elasticity, damping, volume ratio of inter-connected pore structure and permeability based on scaffold structure, so that the effect of these properties on specific purpose may be better understood.

The first TPMS structures was reported by Schwarz et al. (1890). Significant new developments began to emerge from the 1960s after a long period of stagnation and Schoen (1970) studied for NASA whether the surfaces might be of use as space structures. Fascinating study was accomplished by Torquato et al. (2002) to show the interesting types of microstructures that can arise in multifunctional optimization, the researchers maximized the simultaneous transport of heat and electricity in 3D two-phase composites by rigorous optimization methods. Interestingly, they found that the optimal 3D architecture are bicontinuous triply periodic minimal surfaces.

TPMS based structures can also be seen in nature such as butterflies, beetles and other insects (Michielsen and Stavenga, 2008; Galusha et al., 2008). TPMS architectures are attractive candidates for where solid material forms are inadequate. And, it is not surprisingly that TPMS based structures have been received attentions in the recent tissue engineering literature (Yoo, 2011; Melchels et al., 2010). Another important consideration when working with porous structures with micro-architectures is to

determine the mechanical properties of the material used. In this context, it is important to obtain the homogenized properties of porous structures with micro-architectures in general, whether they are used in tissue engineering or fields where structural systems of different scales. By means of homogenization, the behaviors of the systems created by repeating the desired number of units using the unit structure can be modeled appropriately. Defining limits on effective properties obtainable for specific architectures has been an area of intense study in applied mathematics, and applied and computational mechanics (Torquato, 2002; Milton, 2001). (Scott and Cheng, 2007) intentions here is to highlight to determine limits on single effective properties (elasticity, diffusion, conductivity, permeability) that can be attained at a certain porosity or ratio of base materials and how these materials should be organized in three dimensional space to attain the limits. There have also been important studies on the development, production and efficient use of TPMS-based surfaces (Lord, 2003; Wang, 2007; Jung et al., 2007; Yoo, 2011, 2011, 2012, 2012; Rajagopalan and Robb, 2006; Melchels et al., 2010, 2010). Particularly due to the porosity and interconnnected pore structure, TPMS structures have become a very important topic in terms of tissue engineering, and very important studies has been done in this context (Yoo, 2011, 2011, 2012, 2012; Rajagopalan and Robb, 2006; Melchels et al., 2010, 2010). In his studies, Dongjin Yoo has handled a number of methods in detail, through proper manipulation of 3d models to obtain appropriate geometries and to change the porosity within a certain gradient (Yoo, 2011, 2011, 2012, 2012).

Determinations of vibration properties of porous structures are important for two reasons. Firstly, one is use of vibration analysis and measuring techniques, containing vibration and ultrasonic applications (Cowin, 1989; Van der Perre and Lowet, 1996; Buchanan and Gilbert, 2007; Renault et al., 2011), while determining mechanical properties of porous materials. The second is porous structures commonly used in environmental including vibrational applications (Akl and Baz, 2006; Gabrielli et al., 2008; Rangel et al., 2010).

Usage of homogenized material properties and approximate geometries is a widely used method while determination of the mechanical properties of structures with micro architectural details. Along with that, it is more realistic when considering micro architectural properties instead of determining general behaviors according to homogenization techniques in problem types in that micro and nano-scaled properties of a structure important. Developments in Imaging Technology and increases in processor speeds enable one to take problems that involve micro-scaled complex solutions by reverse engineering techniques without geometry and material homogenization. Geometric and material properties in which there are macro-scaled mechanical problems in homogenization techniques differ greatly from micro-scaled solutions in terms of quantitatively and qualitatively. It is possible to compute material quantity by knowing porosity ratio. But, the same situation is not valid for rigidity. Since, rigidity does not only depend on material amount but also configuration of micro architectural details. There were large differences found between Young's modulus of porous structures in macro and micro levels by incorporating micro-architecture details in the analyses (Jaasma et al., 2002; Chevalier et al., 2007; Harrison et al., 2008). The meaning of solutions by taking micro-structural details into consideration was studied by taking compared calculations of numerous problems in different scales (Saxena and Ramakrishnan, 2007). Numerous methods from studies in different scales, including vibro-acoustic techniques, are studied to determine the properties of porous materials, and the topic is also actual. In this context, Renault et al. (2011) studied a technique for dynamic measurement of elasticity modulus and damping of viscoelastic porous materials. The benefits of this method were that the experimental set-up was simple and measurements gave reliable results. Wojtowicki et al. (2004) established a technique, inspired by the Oberst et al. (1985) technique, grounded on transfer function measurement and calculation of a free–free beam excited at its midpoint. Liao and Wells (2008) offered a technique for complex elasticity modulus calculation. In this study, beam shaped models were used for the calculation of porous material parameters due to their simplicity. Related study for plate samples were applied by Jaouen et al. (2005). Mechanical properties of porous structures are typically studied after numerous homogenized applications due to their complex geometric forms. It is known that usage of homogenized properties of micro details in structural analyses provides savings in terms time and computational effort. However, realistic analyses can be achieved by counting micro architectural details, thanks to advancing technology. In this context, modal behaviors of a porous structure are examined by taking microstructural details into consideration according to the voxel-based finite element model, and significant properties, which cannot be observed in routine modal analyses, are determined by Altintas (2013). Furthermore, analyses using the homogenized model of porous structure are studied, and it is seen that the acquired results are not only different numerically but also have different modal behavior from the porous structure.

In this study, vibration behavior of structures formed from TPMS unit cells, in which all the properties of geometry can be controlled by mathematical equations and all the advantages of microporous architecture can be exploited. The TPMS unit cell structures used in this study were different from the analyzes in which the above-mentioned TPMS geometry was made by filling one of the two regions into different regions. TPMS interface was considered as the basic structural carrier system and TPMSs were used with the advantage of optimum forms found in the nature by preserving the labyrinth areas which were separated. Main focus of this study is investigation of the free vibration behavior of TPMS based structures by concentrating on the combination of material and geometry with the highest fabrication potential. In order for the results of the trial to be applicable not only theoretically but also in practice, analyzed beams based on different TPMS geometry, material and thickness are studied in an extensive and realistic ranges.

2. Theoretical Formulation of TPMSs and Modeling Procedure

The surface with zero mean curvature at all points is called the minimal surface. Obtaining a minimal surface for a certain boundary conditions is a subject in the calculus of variations. It is also known as Plateau's problem. There are large class of triply periodic minimal surfaces based on for biomorphic porous scaffold structures with biologically and biomechanically useful properties. In this study, It is studied that triply periodic minimal surfaces as: Θ_P , Θ_G , Θ_{I-WP} , Θ_L , Θ_{F-RD} shows Figure 1.

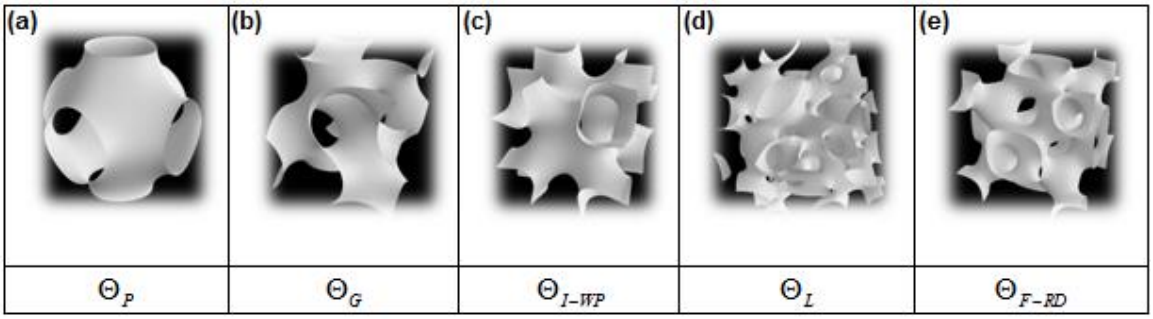

Figure 1. TMPS based unit cells of triply periodic structures.

Studied TPMS surfaces with first order of approximation, by the following nodal equations (Joo, 2012):

$$\Theta_P(x,y,z) = \cos(X) + \cos(Y) + \cos(Z) \quad (1)$$

$$\Theta_G(x,y,z) = \sin(Z)\cos(X) + \sin(X)\cos(Y) + \sin(Y)\cos(Z) \quad (2)$$

$$\Theta_{I-WP}(x,y,z) = 2\left[\cos(X)\cos(Y) + \cos(Y)\cos(Z) + \cos(Z)\cos(X)\right] - \left[\cos(2X) + \cos(2Y) + \cos(2Z)\right] \quad (3)$$

$$\Theta_L(x,y,z) = 0.5\left[\sin(2X)\cos(Y)\sin(Z) + \sin(2Y)\cos(Z)\sin(X) + \sin(2Z)\cos(X)\sin(Y)\right] - 0.5\left[\cos(2X)\cos(2Y) + \cos(2Z)\cos(2Y) + \cos(2X)\cos(2Z)\right] + 0.15 \quad (4)$$

$$\Theta_{F-RD}(x,y,z) = 4\cos(X)\cos(Y)\cos(Z) - \left[\cos(2X)\cos(2Y) + \cos(2X)\cos(2Z) + \cos(2Z)\cos(2Y)\right] \quad (5)$$

where $X = 2\pi x,\ Y = 2\pi y, Z = 2\pi z$.

For the TPMS, the field is taken to be a unit cell of the periodically repeating architecture, as presented in Figure 2. Surface of interest is represented by the zero level set of Θ. The surface splits the unit cell into the two distinct volumes.

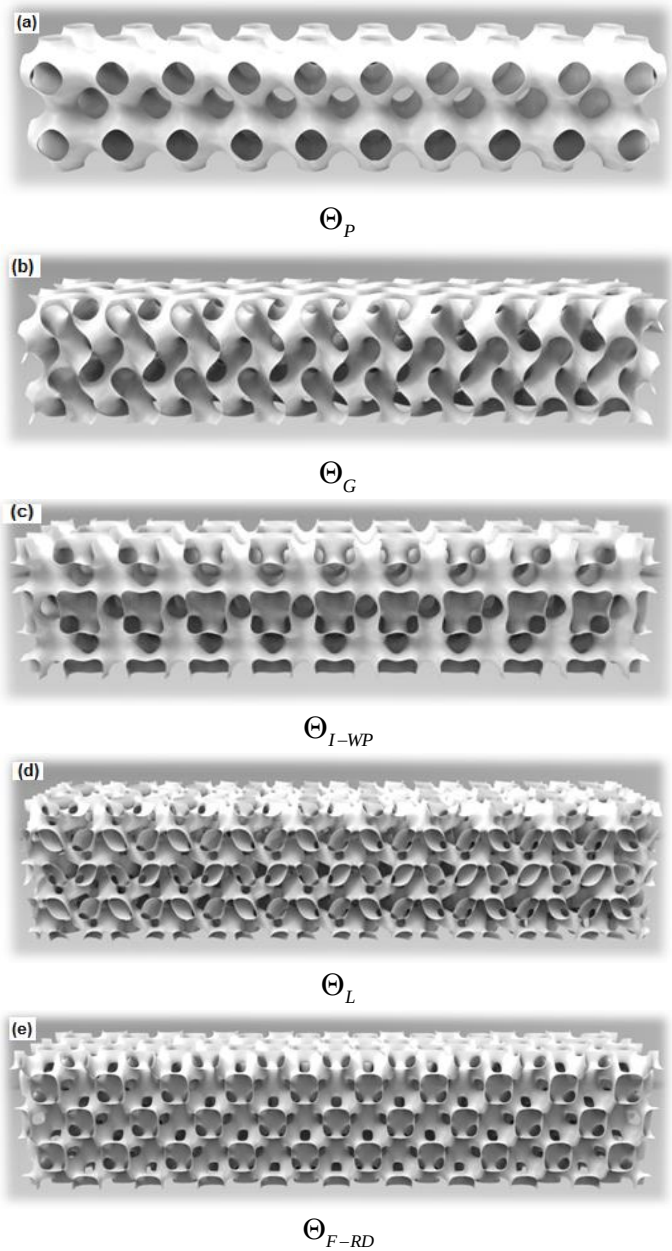

Figure 2. TMPS based beams as periodically repeating structures

In this study, the equations given in Eq (1) are parametrically defined and discretized. Since any position on the surface can be uniquely specified by coordinates, and the surface is said to be parameterized by coordinates. Discretized and triangulazied surfaces were used for obtaining STL geometry files. STL file type can carry knowledge of an unstructured triangulated surface data by the unit normal and vertices of the triangles using a three-dimensional Cartesian coordinate system. The triangular geometry of the discretized surfaces included in the STL files can be introduced directly into many finite element analysis software as Shell elements. The finite element models obtained in the study are obtained by this procedure, but additional considerations must be taken into account. In the process of discerizing mathematical surfaces, the element dimension stability required for the finite element method, and the adjustment of the dimensions required for the shell behavior, may not be

achieved during the surface creation process. For this reason, the finite element meshes of the surfaces in the study have been redesigned to meet the requirements of the finite element method. Thanks to the development of 3D printer technology, the use of high-precision printers such as steel, brass, copper, bronze, sterling silver, gold, platinum, titanium, and aluminum has also become widespread. In this context, the results obtained in this study are not only academic but also easy to understand from the point of view of the practitioners. In order to make the models obtained with the aim steel, titanium and aluminum were analyzed.

3. Numerical Results

It is aimed to investigate TPMS based structures for natural vibration behaviors by focusing on materials with high production potential. In this context steel, titanium and aluminum materials are presented which are characterized by a wide range of practical applications. The properties of the materials are as given in Table 1 and the poisson ratio is taken as 0.3.

Table 1. Material Properties of Analyzed Models

Material	*Young's modulus* (N/mm^2)	*Mass* (t/mm^3)
Steel	200000	7.85e-9
Titanium	100000	4.5e-9
Aluminum	65000	2.75e-9

Since the beam models are obtained from the shell elements and from the STL-based geometry files, after the element size adjustment, the finite element models are created using the S3R type elements directly. The number of points and elements of the TPMS based beam models used in the analyzes are presented in Table 2. All models were obtained through identical procedures except for equations.

Table 2. Basic Mesh Properties of Models

Form	*Number of Nodes*	*Number of Elements*
Θ_{I-WP}	227296	431208
Θ_{L}	401892	760953
Θ_{P}	151213	285146
Θ_{G}	202046	378403
Θ_{F-RD}	304795	582814

The rectangular prism dimensions that they fit into the TPMS-based Beam Models are 13 mm x 13 mm x 65 mm. The natural vibration behavior of the beams presented in figure 3 using the unit geometries (Θ_{P} , Θ_{G} , Θ_{I-WP} , Θ_{L} , Θ_{F-RD}) was obtained for the case of using steel, aluminum, titanium in two different thicknesses.

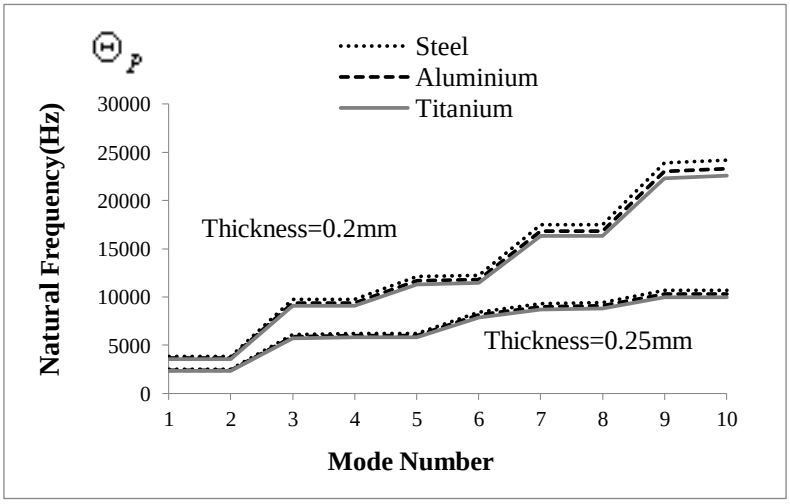

Figure 3. Modal Properties of TMPS based structures (Θ_P) for material types and thickness values

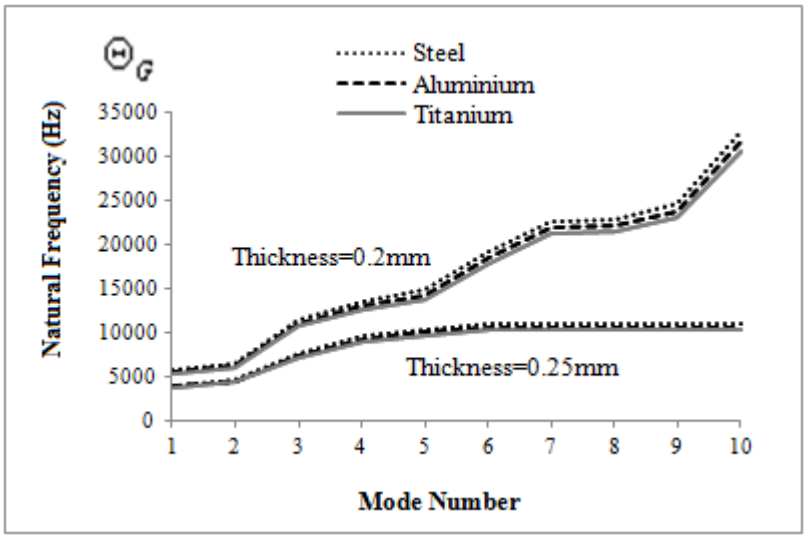

Figure 4. Modal Properties of TMPS based structures (Θ_G) for material types and thickness values

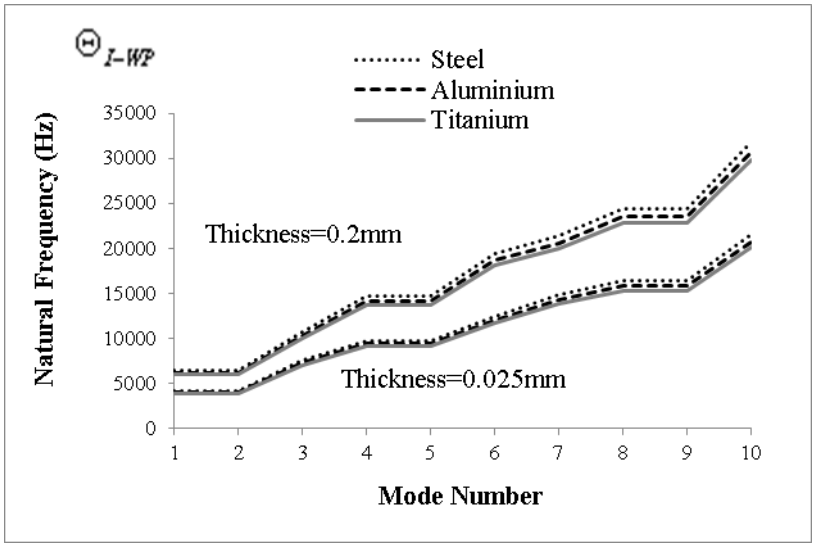

Figure 5. Modal Properties of TMPS based structures (Θ_{I-WP}) for material types and thickness values

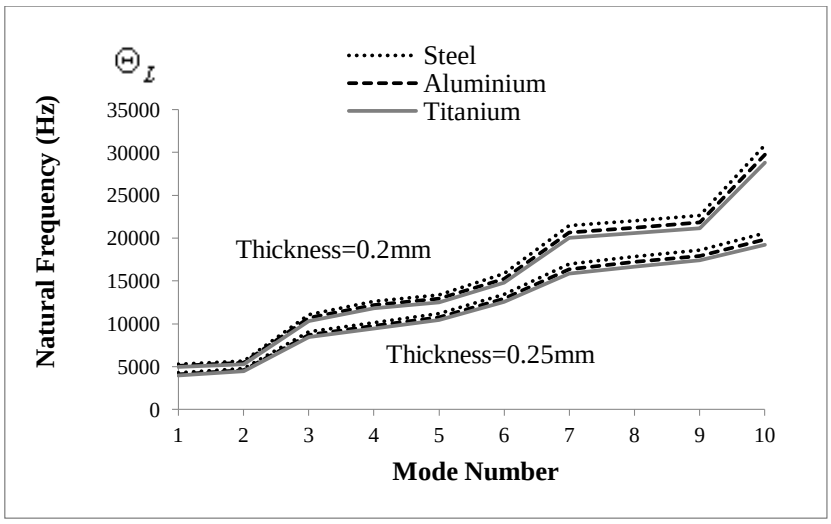

Figure 6. Modal Properties of TMPS based structures (Θ_L) for material types and thickness values

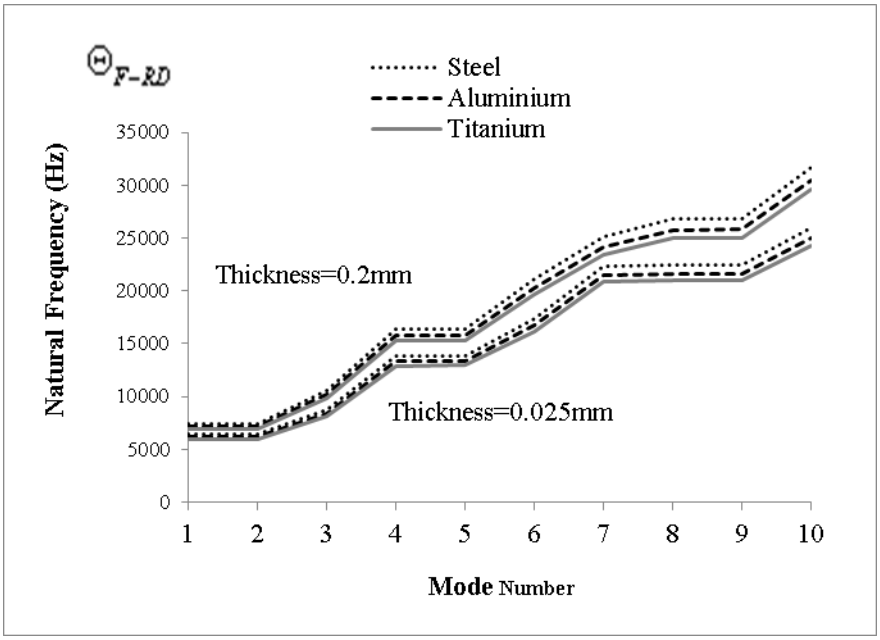

Figure 7. Modal Properties of TMPS based structures (Θ_{F-RD}) for material types and thickness values

When examining the curves presented in Figure 3, it is important to make inferences about the TPMS function, the material type, and the effects of the thickness on the natural vibration behavior. In general, it is known that, in many systems, the increase in mass value decreases the natural frequency value, while the increase in the stiffness value increases the natural frequency value. The increase in thickness brings about the increase in rigidity and mass values. However, since the effects of stiffness and mass values on natural vibration values are different from each other, it is difficult to predict the effect of thickness variation on natural frequency without analyzing. It is also important to determine the effect of the thickness variation on the natural vibration behavior of the different mod types of different TPMS-based beams. The graphs in Figure 3 clearly show that the natural vibrational behavior of the beam configurations examined is significantly influenced by the thickness variation. As the thickness increased, the natural frequency values of all the beam configurations appeared at larger values. The effects on the natural vibration behavior of the thickness, beam configurations are similar. However, this effect was found to be more limited in the beams obtained from Θ_{F-RD} and Θ_L unit cells. In general, the effect of thickness variation on all beam configurations increases with the increase of modes. In other words, thickness adjustment is more important in designs where higher modes require more attention. If the graphical values are to be examined in terms of materials, the steel beams for all beam configurations determine the upper limit of the natural frequency and the titanium beams the lower limit of the natural frequency. Although the natural frequencies of aluminum beams remain between steel and titanium, their mass and modulus values are lower than those of steel and aluminum. In order to better understand the results obtained in this study and to make the results easier to understand, natural frequencies values are presented in tabular form together with mode types in Table 3-7. It is aimed to show whether the order of the mod types has changed or not and how the different mode types are influenced from the examined parameters. In this context, the curves in the graphs correspond to those where the symmetric mode types are horizontal and the modes are separated from each other when there is no symmetry in the unit cell from which the TPMS is obtained. In this case, it is easily detected that the TPMS which is composed of unit cell of type Θ_G and Θ_L is different from other TPMS which are symmetrical with respect to the beam axes, such as mode separation which is included in Table 3-7 in the mod type.

Table 3. Modal Properties of Θ_{I-WP} based structures for material types and thickness values

Θ_{I-WP}

Wall Thickness of Aluminum (mm)						
Mode Number	0.025	0.05	0.1	0.15	0.2	Mode Type
1	3931.744	4622.718	5340.076	5784.998	6109.508	Bending1 (a, b)
2	7239.211	8372.229	9468.775	9988.082	10301.81	Torsional 1
3	9370.676	10946.65	12511.85	13440.53	14099.45	Bending2 (a, b)
4	11996.33	14302.63	16375.06	17692.79	18725.36	Longitudinal
5	14237.9	16612.9	18857.18	19911.98	20550.11	Torsional 2
6	15755.57	18442.44	21015.06	22501.48	23541.92	Bending3 (a, b)
7	20682.21	24580.24	28081.57	29703.93	30688.46	Torsional 3
Wall Thickness of Steel (mm)						
Mode Number	0.025	0.05	0.1	0.15	0.2	Mode Type
1	4082.019	4799.403	5544.179	6006.107	6343.021	Bending1 (a, b)
2	7515.901	8692.225	9830.682	10369.840	10695.550	Torsional 1
3	9728.833	11365.050	12990.060	13954.240	14638.340	Bending2 (a, b)
4	12454.839	14849.290	17000.930	18369.030	19441.070	Longitudinal
5	14782.085	17247.860	19577.920	20673.040	21335.560	Torsional 2
6	16357.763	19147.330	21818.280	23361.520	24441.720	Bending3 (a, b)
7	21472.705	25519.720	29154.880	30839.250	31861.410	Torsional 3
Wall Thickness of Titanium (mm)						
Mode Number	0.025	0.05	0.1	0.15	0.2	Mode Type
1	3812.314	4482.299	5177.866	5609.274	5923.927	Bending1 (a, b)
2	7019.314	8117.915	9181.152	9684.685	9988.881	Torsional 1
3	9086.033	10614.14	12131.79	13032.26	13671.16	Bending2 (a, b)
4	11631.93	13868.18	15877.65	17155.36	18156.56	Longitudinal
5	13805.41	16108.27	18284.38	19307.14	19925.88	Torsional 2
6	15276.98	17882.23	20376.71	21817.98	22826.82	Bending3 (a, b)
7	20053.97	23833.59	27228.57	28801.65	29756.28	Torsional 3

Table 4. Modal Properties of Θ_{F-RD} based structures for material types and thickness values

Θ_{F-RD}

Wall Thickness of Aluminum (mm)						
Mode Number	0.025	0.05	0.1	0.15	0.2	Mode Type
1	6137.85	6411.578	6732.68	6972.382	7171.134	Bending1 (a, b)
2	8357.949	8772.474	9297.266	9747.695	10158.45	Torsional 1
3	13321.8	13936.11	14677.42	15258.99	15757.92	Bending2 (a, b)
4	16691.94	17536.15	18594.96	19499.1	20322.17	Torsional 2
5	21511.56	22349.29	23258.68	23808.57	24199.06	Longitudinal
6	21629.84	22668.32	23923.35	24921.09	25786.08	Bending3 (a, b)
7	24969.43	26275.81	27888.8	29254.18	30493.33	Torsional 3
Wall Thickness of Steel (mm)						
Mode Number	0.025	0.05	0.1	0.15	0.2	Mode Type
1	6372.445313	6656.636	6990.01	7238.874	7445.222	Bending1 (a, b)
2	8677.399414	9107.768	9652.617	10120.26	10546.72	Torsional 1
3	13830.97461	14468.76	15238.4	15842.2	16360.2	Bending2 (a, b)
4	17329.91797	18206.4	19305.68	20244.38	21098.9	Torsional 2
5	22333.75195	23203.51	24147.65	24718.56	25123.97	Longitudinal
6	22456.55078	23534.72	24837.72	25873.6	26771.65	Bending3 (a, b)
7	25923.78906	27280.1	28954.74	30372.31	31658.82	Torsional 3
Wall Thickness of Titanium (mm)						
Mode Number	0.025	0.05	0.1	0.15	0.2	Mode Type
1	5951.408	6216.821	6528.169	6760.59	6953.304	Bending1 (a, b)
2	8104.069	8506.002	9014.853	9451.601	9849.882	Torsional 1
3	12917.14	13512.79	14231.58	14795.48	15279.26	Bending2 (a, b)
4	16184.9	17003.47	18030.12	18906.8	19704.87	Torsional 2
5	20858.13	21670.42	22552.18	23085.37	23463.99	Longitudinal
6	20972.81	21979.75	23196.65	24164.09	25002.81	Bending3 (a, b)
7	24210.96	25477.66	27041.66	28365.56	29567.07	Torsional 3

Table 5. Modal Properties of Θ_G based structures for material types and thickness values

Θ_G

	Wall Thickness of Aluminum (mm)					
Mode Number	0.025	0.05	0.1	0.15	0.2	Mode Type
1	3845.464	4399.827	4935.227	5228.672	5433.099	Bending1 a
2	4471.654	5122.511	5662.102	5930.381	6103.776	Bending1b
3	7222.271	8616.117	9919.544	10610.224	11072.358	Torsional 1
4	9147.849	10574.582	11824.612	12493.275	12958.766	Bending2 a
5	9994.599	11789.478	13130.966	13776.376	14190.052	Bending2b
6	15047.428	16137.944	17384.937	18005.885	18417.731	Longitudinal
7	14003.028	16202.077	19354.935	20846.749	21816.735	Torsional 2
	Wall Thickness of Steel (mm)					
Mode Number	0.025	0.05	0.1	0.15	0.2	Mode Type
1	3992.441	4567.993	5123.857	5428.518	5640.758	Bending1 a
2	4642.565	5318.299	5878.513	6157.047	6337.063	Bending1b
3	7498.313	8945.435	10298.68	11015.75	11495.55	Torsional 1
4	9497.489	10978.75	12276.56	12970.78	13454.05	Bending2 a
5	10376.6	12240.07	13632.83	14302.92	14732.41	Bending2b
6	15621.58	16754.75	18049.4	18694.09	19121.68	Longitudinal
7	14538.37	16821.33	20094.69	21643.53	22650.59	Torsional 2
	Wall Thickness of Titanium (mm)					
Mode Number	0.025	0.05	0.1	0.15	0.2	Mode Type
1	3728.654	4266.178	4785.315	5069.847	5268.063	Bending1 a
2	4335.823	4966.91	5490.11	5750.241	5918.363	Bending1b
3	7002.888	8354.396	9618.229	10287.92	10736.02	Torsional 1
4	8869.975	10253.37	11465.43	12113.78	12565.12	Bending2 a
5	9691.004	11431.35	12732.09	13357.9	13759.01	Bending2b
6	14589.5	15647.74	16856.84	17458.94	17858.28	Longitudinal
7	13577.8	15709.91	18767	20213.5	21154.03	Torsional 2

Table 6. Modal Properties of Θ_L based structures for material types and thickness values

Θ_L

Wall Thickness of Aluminum (mm)						
Mode Number	0.025	0.05	0.1	0.15	0.2	Mode Type
1	4106.178	4383.929	4701.76	4927.451	5117.023	Bending1 a
2	4587.305	4826.107	5105.574	5308.65	5479.438	Bending1b
3	8727.396	9289.146	9903.432	10328.07	10674.86	Torsional 1
4	9758.343	10431.22	11192.01	11728.6	12176.35	Bending2 a
5	10761.7	11348.73	12024.53	12509.94	12915.37	Bending2b
6	12937.68	13508.45	14223.51	14781.03	15273.79	Longitudinal
7	16339.1	17636.24	18970.02	19895.16	20661.09	Bending3 a
8	17945.6	19119.45	20307.53	21146.57	21842.93	Bending3b
9	17220	18411.28	19670.18	20531.05	21231.48	Torsional 2
Wall Thickness of Steel (mm)						
Mode Number	0.025	0.05	0.1	0.15	0.2	Mode Type
1	4263.120117	4551.488	4881.466	5115.783	5312.602	Bending1 a
2	4762.637207	5010.566	5300.714	5511.553	5688.869	Bending1b
3	9060.96582	9644.188	10281.95	10722.82	11082.86	Torsional 1
4	10131.31738	10829.91	11619.78	12176.88	12641.74	Bending2 a
5	11173.02734	11782.49	12484.12	12988.08	13409.01	Bending2b
6	13432.17285	14024.75	14767.15	15345.98	15857.57	Longitudinal
7	16963.59375	18310.32	19695.07	20655.58	21450.78	Bending3 a
8	18631.49609	19850.21	21083.7	21954.81	22677.79	Bending3b
9	17878.16406	19114.98	20421.99	21315.77	22042.97	Torsional 2
Wall Thickness of Titanium (mm)						
Mode Number	0.025	0.05	0.1	0.15	0.2	Mode Type
1	3981.449	4250.764	4558.939	4777.775	4961.589	Bending1 a
2	4447.962	4679.51	4950.488	5147.396	5312.996	Bending1b
3	8462.293	9006.98	9602.605	10014.35	10350.6	Torsional 1
4	9461.925	10114.36	10852.04	11372.33	11806.48	Bending2 a
5	10434.81	11004	11659.27	12129.94	12523.05	Bending2b
6	12544.69	13098.12	13791.46	14332.04	14809.83	Longitudinal
7	15842.78	17100.52	18393.79	19290.83	20033.49	Bending3 a
8	17400.48	18538.68	19690.67	20504.22	21179.43	Bending3b
9	16696.93	17852.02	19072.68	19907.4	20586.55	Torsional 2

Table 7. Modal Properties of Θ_P based structures for material types and thickness values

Θ_P

Wall Thickness of Aluminum (mm)

Mode Number	0.025	0.05	0.1	0.15	0.2	Mode Type
1	2415.28	2729.409	3110.01	3406.171	3673.652	Bending1 (a, b)
2	6006.44	6902.271	7954.519	8720.135	9384.361	Bending2 (a, b)
3	5869.56	7780.197	9801.768	10932.54	11676.13	Torsional 1
4	8969.74	9962.093	10777.02	11320.01	11814.37	Longitudinal
5	10291.4	12139.77	14241.24	15667.77	16849.92	Bending3 (a, b)
6	10628.9	14648.61	19017.33	21449.93	23029.43	Torsional 2

Wall Thickness of Steel (mm)

Mode Number	0.025	0.05	0.1	0.15	0.2	Mode Type
1	2507.599121	2833.73	3228.877	3536.358	3814.063	Bending1 (a, b)
2	6236.012207	7166.083	8258.549	9053.428	9743.042	Bending2 (a, b)
3	6093.898926	8077.564	10176.4	11350.39	12122.4	Torsional 1
4	9312.572266	10342.85	11188.93	11752.68	12265.93	Longitudinal
5	10684.75098	12603.77	14785.55	16266.61	17493.94	Bending3 (a, b)
6	11035.11035	15208.5	19744.2	22269.77	23909.64	Torsional 2

Wall Thickness of Titanium (mm)

Mode Number	0.025	0.05	0.1	0.15	0.2	Mode Type
1	2341.918	2646.5	3015.54	3302.705	3562.062	Bending1 (a, b)
2	5823.989	6692.608	7712.894	8455.253	9099.304	Bending2 (a, b
3	5691.265	7543.866	9504.03	10600.45	11321.46	Torsional 1
4	8697.276	9659.485	10449.66	10976.16	11455.5	Longitudinal
5	9978.792	11771.01	13808.65	15191.85	16338.09	Bending3 (a. b)
6	10306	14203.65	18439.66	20798.37	22329.89	Torsional 2

The natural frequency values in Table 3-7 are obtained for TPMS thickness interim values and for all three material types. It is clear that the effect of the thickness variation on the natural frequency values is not linear due to the complexity of the effect on stiffness and the mass. In addition, the influence of thickness and material changes on different mode types is different. This effect can be large enough to change modal ordering in thin-walled beams. This was observed in the range of the Logitudional-1 and Torsional-2 modes of the Θ_G type TPMS with a thickness of only 0.025 mm in the investigation interval. A similar situation is observed in the Θ_P unit cell-based TPMS, which is observed in the order of Torsional-1 and Bending-2 modes of the beams with a thickness of 0.025 mm. In Θ_L, Torsional-2 modes for all thickness values appeared between the separated parts of Bending-3 modes.

4. Results and Conclusions

In this study, free vibration behaviors of beams formed from different TPMS unit cells are investigated for various material and wall-thickness values. Materials and other variables used in the study were

selected in accordance with the values for the parametric examination as well as for the practical purposes. The free vibration analysis is included in the higher modes and the analysis results include the numerical values of the modes as well as the mod types.

The results obtained in the study can be summarized as follows.

- As mentioned above, the stiffness and mass values, which have different effects on the natural vibration behavior, are directly affected by the thickness variation. For this reason, important results have been drawn from the examination of the range of wall-thickness and the complex relationship between the natural vibration behavior of TPMS-based beams. The results showed that wall thickness increases in all beam configurations caused natural vibration modes to appear at higher values. In other words, the effect of the increase in thickness on the rigidity is greater than the effect on the mass.
- The effect of thickness variation on high modes is much greater than the effect on low modes. For this reason, it is more important to select the appropriate thickness values when the forced vibration values are close to the vibration values of the high modes.
- There are great differences in the natural vibration behavior of the beams obtained from different unit cells due to the thickness variation. This effect is particularly large in beams made from a certain unit cells, which is large enough to change the order of the modes at low values of the wall thickness. This can be a great advantage in the design of TPMS-based beams that will be subject to vibration in use when well managed.
- The overlapping modes of the beams produced from the symmetrical unit cells appear to be separated as expected in the beams produced from the unsymmetrical unit cells.
- The effects of material types on natural vibration behavior are similar for all thicknesses and unit cell types. The order of the natural frequency values of the beams produced from different materials arises in a different order than the order of the Young's modulus and mass values.

The results of the study showed that the TPMS-based structures with various interesting tunable parameters as well as material and wall thickness for the familiar adjustments can be tailored to suit a variety of needs.

References

Akl, W., & Baz, A. (2006). Active vibration and noise control using smart foam. Journal of Vibration and Control, 12(11), 1173-1203.

Altintas, G. (2014). Natural vibration behaviors of heterogeneous porous materials in micro scale. Journal of Vibration and Control, 20(13), 1999-2005.

Buchanan, J. L., & Gilbert, R. P. (2007). Determination of the parameters of cancellous bone using high frequency acoustic measurements. Mathematical and Computer Modelling, 45(3), 281-308.

Chevalier, J., Gremillard, L., & Deville, S. (2007). Low-temperature degradation of zirconia and implications for biomedical implants. Annu. Rev. Mater. Res., 37, 1-32.

Cowin, S. C., & Mehrabadi, M. M. (1989). Identification of the elastic symmetry of bone and other materials. Journal of biomechanics, 22(6-7), 503-515.

Gabrielli, F., Guillemain, P., Ogam, E., & Masson, C. (2008). Bone integrity described by resonance frequency signature. Computer Methods in Biomechanics and Biomedical Engineering, 11(S1), 95-96.

Galusha, J. W., Richey, L. R., Gardner, J. S., Cha, J. N., & Bartl, M. H. (2008). Discovery of a diamond-based photonic crystal structure in beetle scales. Physical Review E, 77(5), 050904.

Harrison, R., Jaumandreu, J., Mairesse, J., & Peters, B. (2008). Does innovation stimulate employment A firm-level analysis using comparable micro-data from four European countries (No. w14216). National Bureau of Economic Research.

Hollister, S. J., & Lin, C. Y. (2007). Computational design of tissue engineering scaffolds. Computer methods in applied mechanics and engineering, 196(31), 2991-2998.

Jaasma, M. J., Bayraktar, H. H., Niebur, G. L., & Keaveny, T. M. (2002). Biomechanical effects of intraspecimen variations in tissue modulus for trabecular bone. Journal of biomechanics, 35(2), 237-246.

Jaouen, L., Brouard, B., Atalla, N., & Langlois, C. (2005). A simplified numerical model for a plate backed by a thin foam layer in the low frequency range. Journal of Sound and Vibration, 280(3), 681-698.

Jung, Y., Chu, K. T., & Torquato, S. (2007). A variational level set approach for surface area minimization of triply-periodic surfaces. Journal of Computational Physics, 223(2), 711-730.

Liao, Y., & Wells, V. (2008). Estimation of complex Young's modulus of non-stiff materials using a modified Oberst beam technique. Journal of Sound and Vibration, 316(1), 87-100.

Lord, E. A., & Mackay, A. L. (2003). Periodic minimal surfaces of cubic symmetry. Current Science, 85(3), 346-362.

Milton, G. (2001). The Theory of Composites, Cambridge University.

Melchels, F. P., Barradas, A. M., Van Blitterswijk, C. A., De Boer, J., Feijen, J., & Grijpma, D. W. (2010). Effects of the architecture of tissue engineering scaffolds on cell seeding and culturing. Acta biomaterialia, 6(11), 4208-4217.

Melchels, F. P., Bertoldi, K., Gabbrielli, R., Velders, A. H., Feijen, J., & Grijpma, D. W. (2010). Mathematically defined tissue engineering scaffold architectures prepared by stereolithography. Biomaterials, 31(27), 6909-6916.

Michielsen, K., & Stavenga, D. G. (2008). Gyroid cuticular structures in butterfly wing scales: biological photonic crystals. Journal of The Royal Society Interface, 5(18), 85-94.

Rangel JH, Rivera AL and Castano VM (2010) Modal behaviour of bones during fracture. Computer Methods in Biomechanics and Biomedical Engineering 13(1): 91–95.

Rajagopalan, S., & Robb, R. A. (2006). Schwarz meets Schwann: design and fabrication of

biomorphic and durataxic tissue engineering scaffolds. Medical Image Analysis, 10(5), 693-712.

Renault, A., Jaouen, L., & Sgard, F. (2011). Characterization of elastic parameters of acoustical porous materials from beam bending vibrations. Journal of Sound and Vibration, 330(9), 1950-1963

Saxena, S., & Ramakrishnan, N. (2007). A comparison of micro, meso and macroscale FEM analysis of ductile fracture in a CT specimen (mode I). Computational materials science, 39(1), 1-7.

Schwarz, H. (1890). Uber Minimalflachen, Monatsber. Berlin Akad.; April 1864; Gesammelte Mathematische Abhandlungen, vol. 1.

Schoen, A. H. (1970). Infinite periodic minimal surfaces without self-intersections.

Torquato, S. (2002). Statistical description of microstructures. Annual review of materials research, 32(1), 77-111.

Torquato, S., Hyun, S., & Donev, A. (2002). Multifunctional composites: optimizing microstructures for simultaneous transport of heat and electricity. Physical review letters, 89(26), 266601.

Van der Perre, G., & Lowet, G. (1996). In vivo assessment of bone mechanical properties by vibration and ultrasonic wave propagation analysis. Bone, 18(1), S29-S35.

Wang, Y. (2007). Periodic surface modeling for computer aided nano design. Computer-Aided Design, 39(3), 179-189.

Wojtowicki, J. L., Jaouen, L., & Panneton, R. (2004). New approach for the measurement of damping properties of materials using the Oberst beam. Review of scientific instruments, 75(8), 2569-2574.

Yoo, D. J. (2011). Computer-aided porous scaffold design for tissue engineering using triply periodic minimal surfaces. International Journal of Precision Engineering and Manufacturing, 12(1), 61-71.

Yoo, D. (2012). Heterogeneous minimal surface porous scaffold design using the distance field and radial basis functions. Medical engineering & physics, 34(5), 625-639.

Yoo, D. J. (2012). Heterogeneous porous scaffold design for tissue engineering using triply periodic minimal surfaces. International Journal of Precision Engineering and Manufacturing, 13(4), 527-537.